Data-driven modeling of the magnetic flux rope: from birth to death

Jinhan Guo

KU Leuven & Nanjing University
Jinhan.guo@kuleuven.be

Yang Guo, Pengfei Chen, Yiwei Ni @ Nanjing University
Stefaan Poedts, Brigitte Schmieder @ KU Leuven
Chun Xia @ Yunnan University; Ze Zhong@Shandong University

EGU meeting, April, 23-29, 2023
Vienna, Austria

Introduction and motivation

Solar corona:
filaments, hot channels and sigmoids

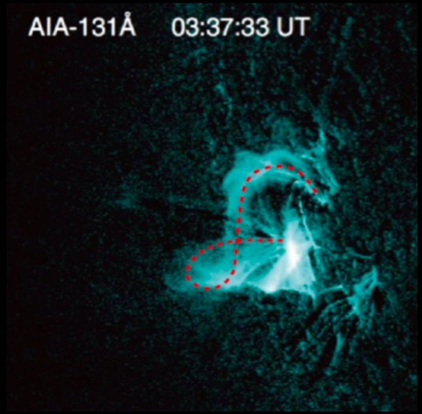

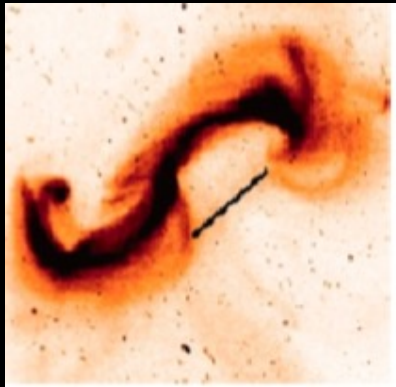

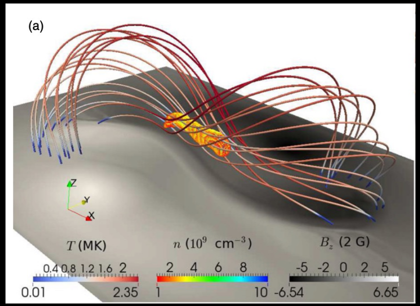

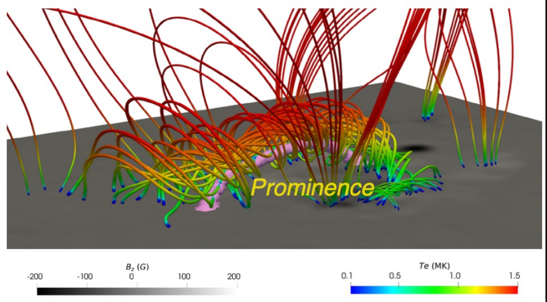

Zhang et al (2012); McKenzie & Canfield et al (2008)
Xia et al (2014); Guo et al (2023)

Interplanetary space:
ICMEs and magnetic clouds

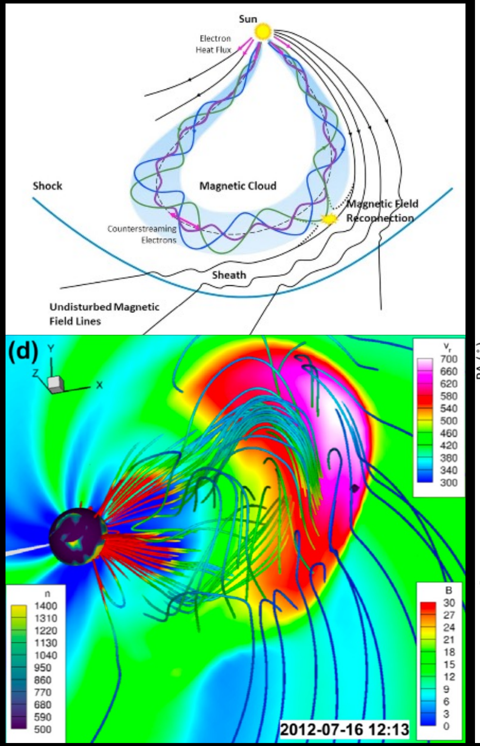

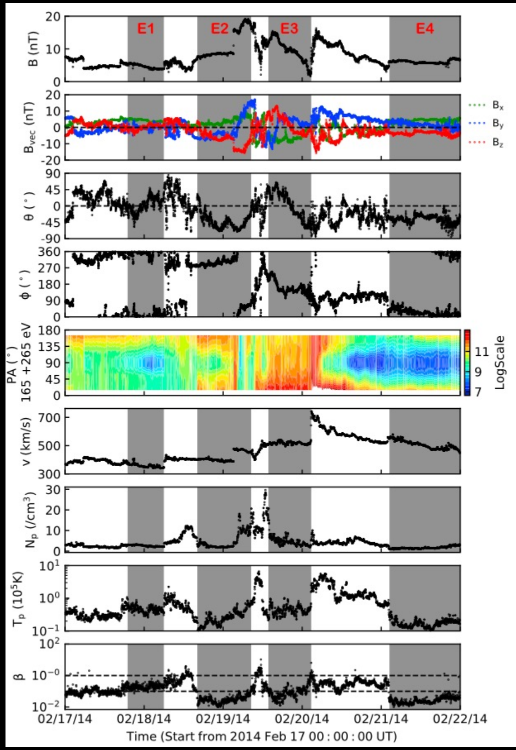

Wang et al (2017); Maharana et al (2022)

Magnetic flux ropes are fundamental magnetic structures in the solar atmosphere and interplanetary spaces, which are the core of CMEs/ICMEs, and major drivers of geomagnetic storms.

Introduction and motivation

To predict the adverse space weather events, we need to develop the observational data-based MHD models.

The aim of this work:

We develop a new data-driven model, to cover the whole process of a flux rope from the formation to eruption.

Numerical strategy

To simulate the two stages of a flux rope in different timesacles, inluding the formation (hours or days) and eruption (seconds and minutes), we combine the time-dependent magnetofrictional method and radiative MHD model.

- Initial magnetic field: potential fields
- Data-driven boundary: vector magnetic fields and velocity fields in the observations
- Quasi-static long-term evolution: time-dependent magnetofrictional method
- Rapid eruption stage: radiative MHD model

Numerical results

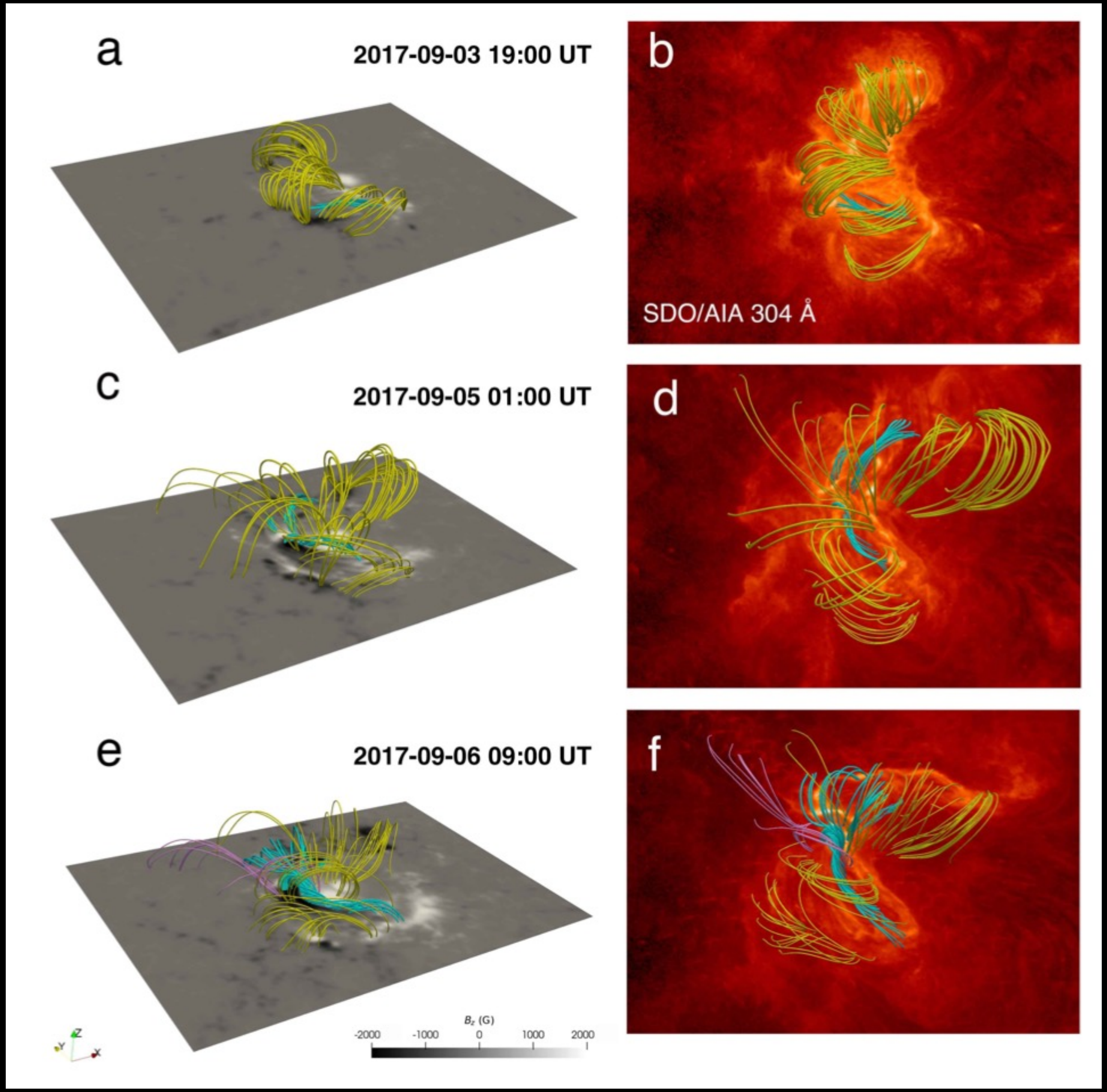

Our simulation retrieves the long-term evolution of the coronal magnetic fields (over three days).

Some key topologies in the observations are simulated:

- Sheared loops
- Formation of the flux rope
- Null points alongside the flux rope

Numerical results

Formation of the flux rope

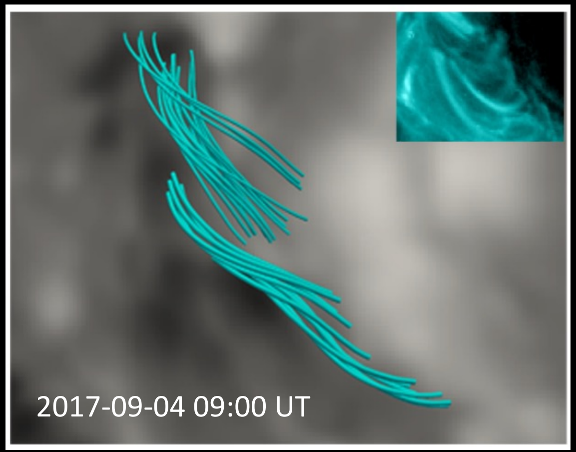

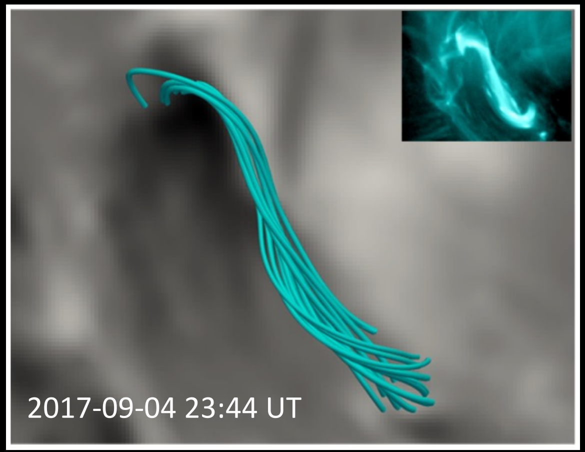

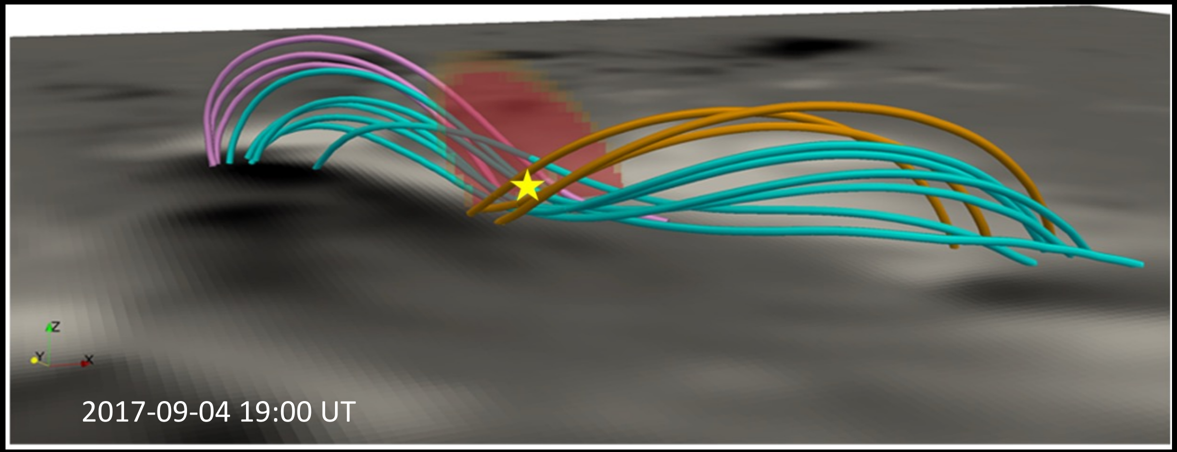

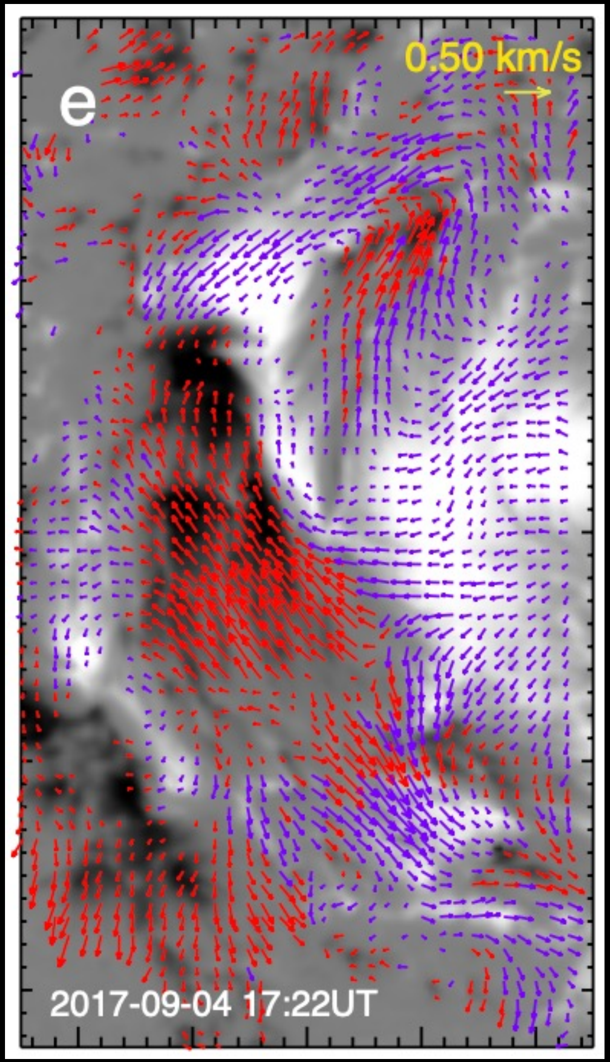

- The flux rope that is in line with the observed hot channel is formed due to the tether-cutting reconnection.
- Shearing and converging plasma flows play a critical role in forming the flux rope

Numerical results

Eruption of the flux rope

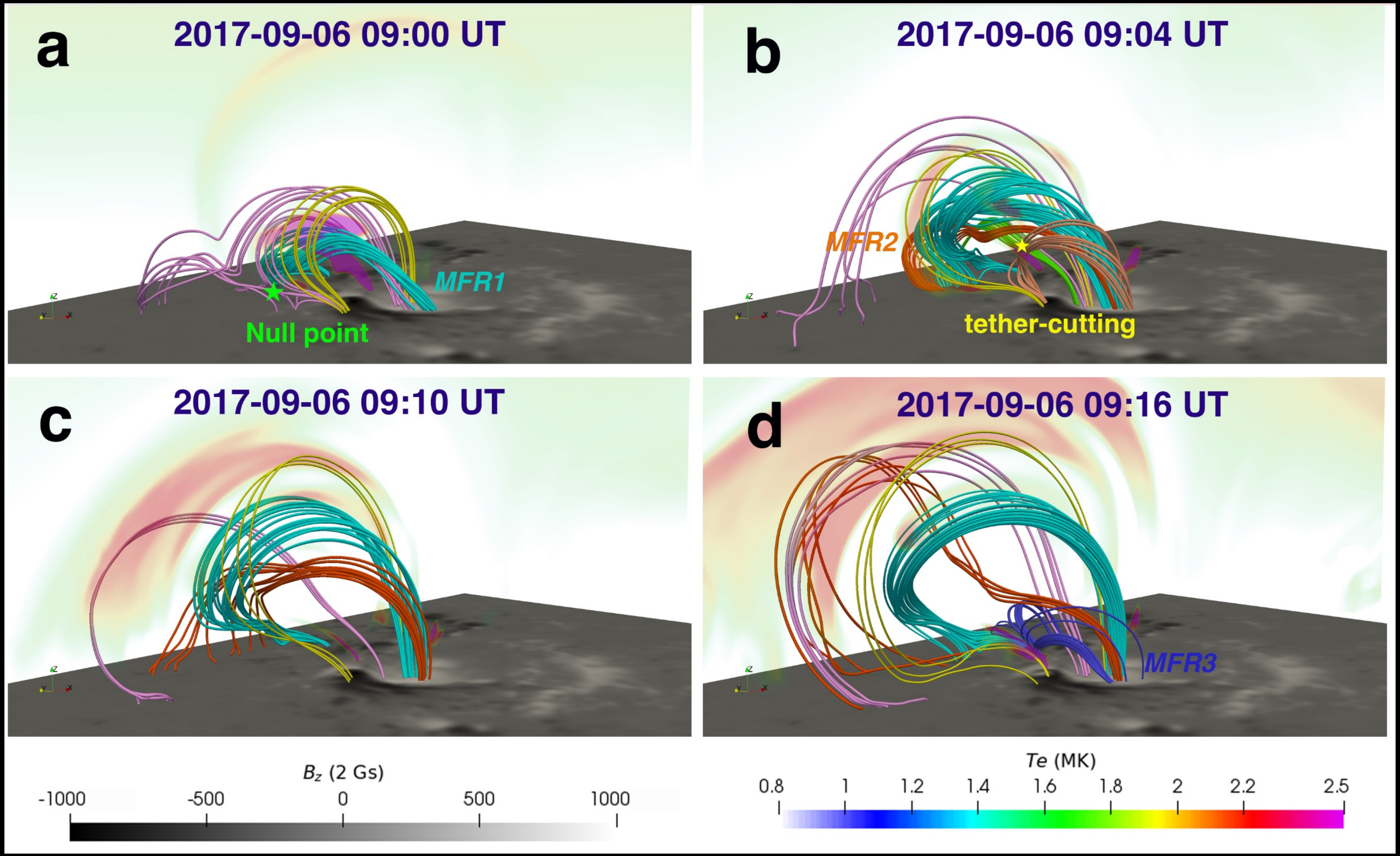

- Null point reconnection triggers the eruption.
- Many flux-rope branches are formed during the eruption

Numerical results

Eruption of the flux rope

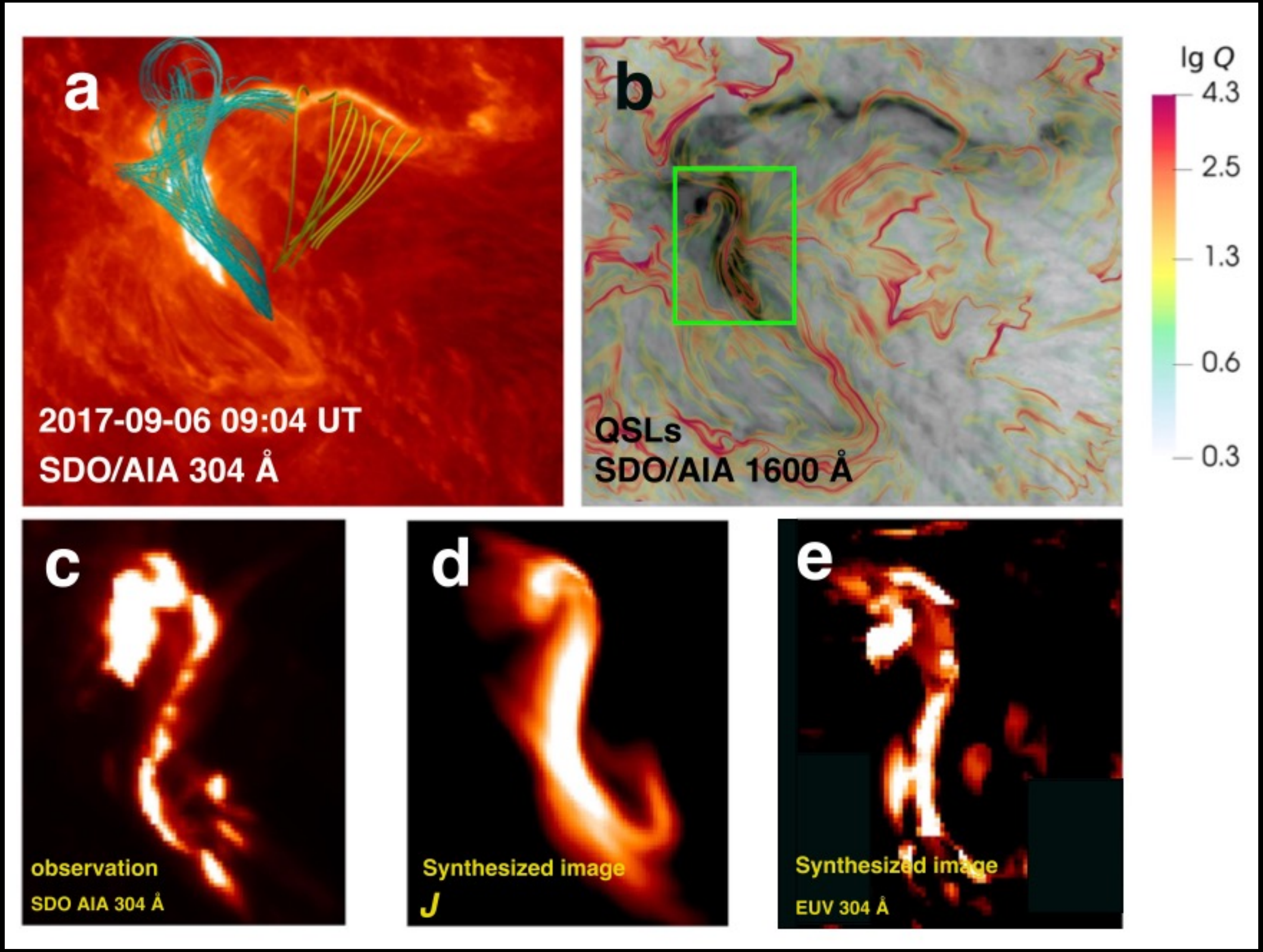

The simulation results are comparable to observations.:

- Erupting structure
- QSLs and flare ribbons.
- Synthesized images

Numerical results

Eruption of the flux rope

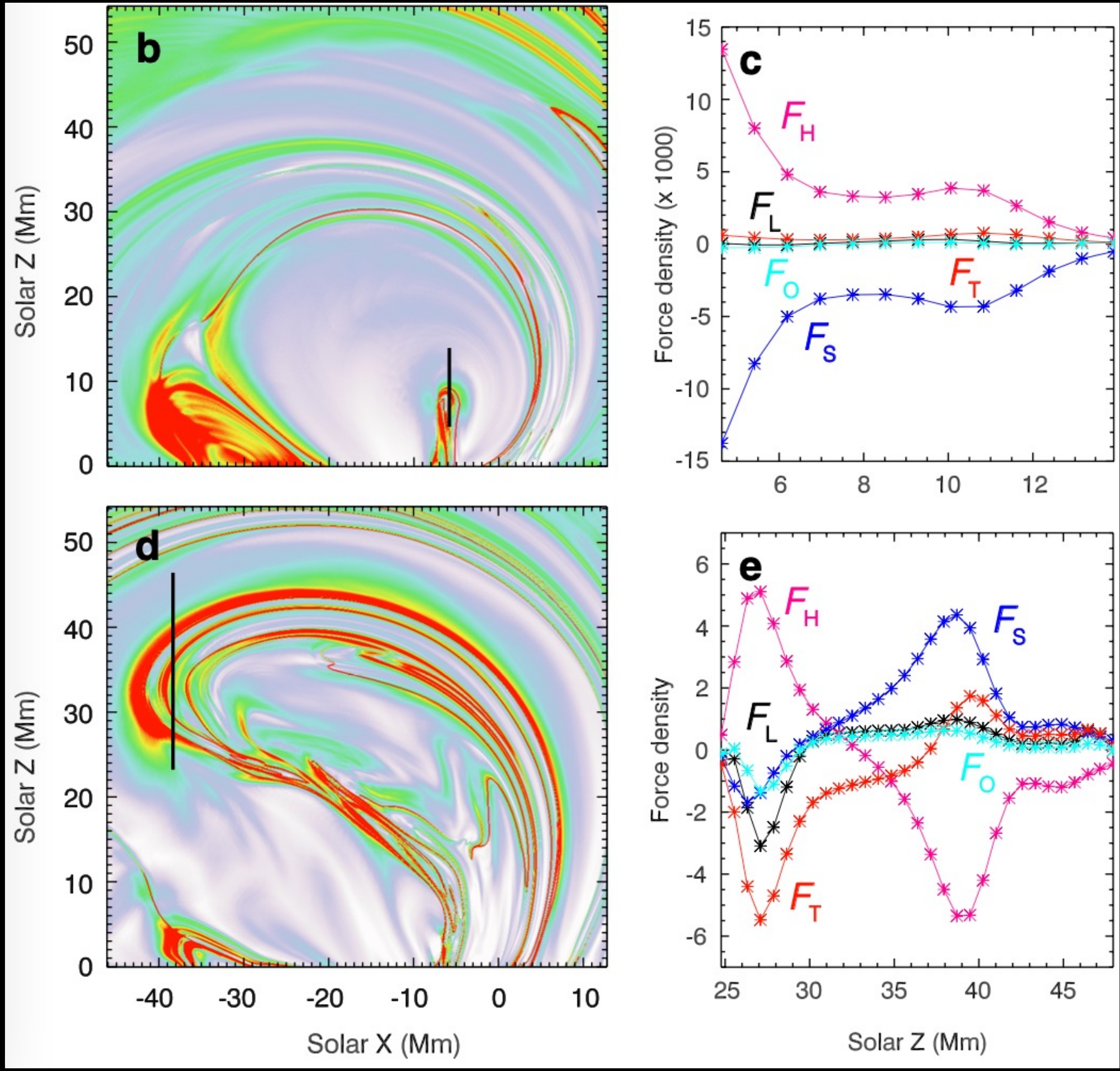

- Dynamic tension force originating from the toroidal (axial) magnetic fields plays a critical role in the confined eruption.
- The deformation and rotation of a flux rope can significantly influence whether it can erupt successfully.

Summary

- We develop a new data-driven model combining the time-dependent magnetofrictional model and radiative MHD model, which can simulate the whole process of a flux rope, from birth to death.
- The shearing and converging plasma flows play a critical role in the formation of the flux rope.
- The deformation and rotation of a flux rope may lead to an increase in dynamic tension force, which will cause the failed eruption.

Thank you for your attention!

Observational event overview

Active region 12673

Table 1
List of All 4 X-class and 27 M-class Flares in AR 12673

Date (UT)	*GOES* Class	Time (UT) Start	Peak	End	Duration (minutes)
2017 Sep 4	M1.2	05:36	05:49	06:05	29
2017 Sep 4	M1.5	15:11	15:30	15:33	22
2017 Sep 4	M1.0	18:05	18:22	18:31	26
2017 Sep 4	M1.7	18:46	19:37	19:52	66
2017 Sep 4	M1.5	19:59	20:02	20:06	7
2017 Sep 4	M5.5	20:28	20:33	20:37	9
2017 Sep 4	M2.1	22:10	22:14	22:19	9
2017 Sep 5	M4.2	01:03	01:08	01:11	8
2017 Sep 5	M1.0	03:42	03:51	04:04	22
2017 Sep 5	M3.2	04:33	04:53	05:07	34
2017 Sep 5	M3.8	06:33	06:40	06:43	10
2017 Sep 5	M2.3	17:37	17:43	17:51	14
2017 Sep 6	X2.2	08:57	09:10	09:17	20
2017 Sep 6	X9.3	11:53	12:02	12:10	17
2017 Sep 6	M2.5	15:51	15:56	16:03	12
2017 Sep 6	M1.4	19:21	19:30	19:35	14
2017 Sep 6	M1.2	23:33	23:39	23:44	11
2017 Sep 7	M2.4	04:59	05:02	05:08	9
2017 Sep 7	M1.4	09:49	09:54	09:58	9
2017 Sep 7	M7.3	10:11	10:15	10:18	7
2017 Sep 7	X1.3	14:20	14:36	14:55	33
2017 Sep 7	M3.9	23:50	23:59	00:14	24
2017 Sep 8	M1.3	02:19	02:24	02:29	10
2017 Sep 8	M1.2	03:39	03:43	03:45	6
2017 Sep 8	M8.1	07:40	07:49	07:58	18
2017 Sep 8	M2.9	15:09	15:47	16:04	55
2017 Sep 8	M2.1	23:33	23:45	23:56	23
2017 Sep 9	M1.1	04:14	04:28	04:43	29
2017 Sep 9	M3.7	10:50	11:04	11:42	52
2017 Sep 9	M1.1	22:04	23:53	00:41	157
2017 Sep 10	X8.2	15:35	16:06	16:31	56

4 X-class and 27 M-class flares

Proxy of the flux-rope formation:

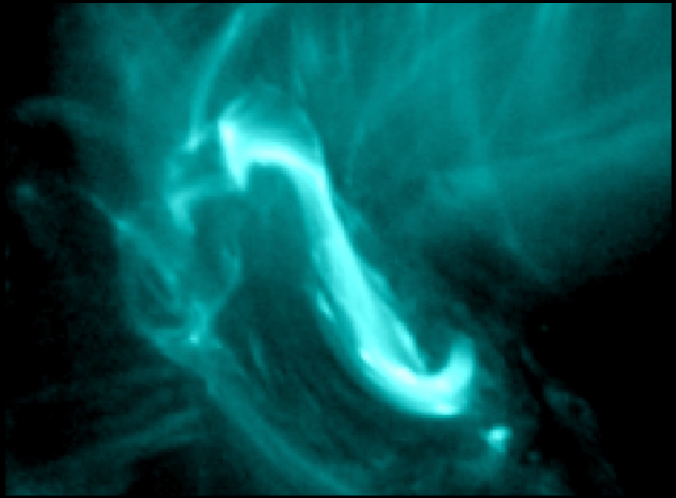

X2.2 confined flare:

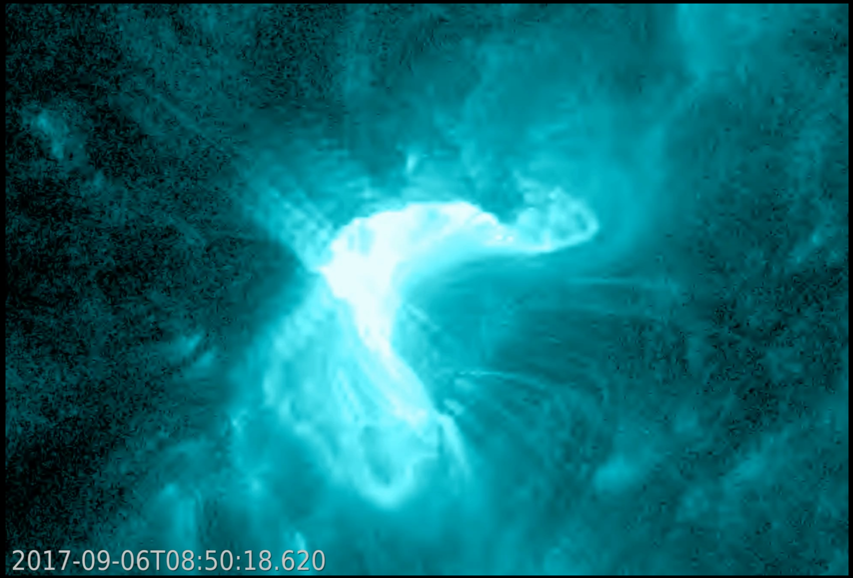

MHD modeling setup

Data-driven boundary

Driven boundary:

Magnetic field + velocity fields in the photosphere

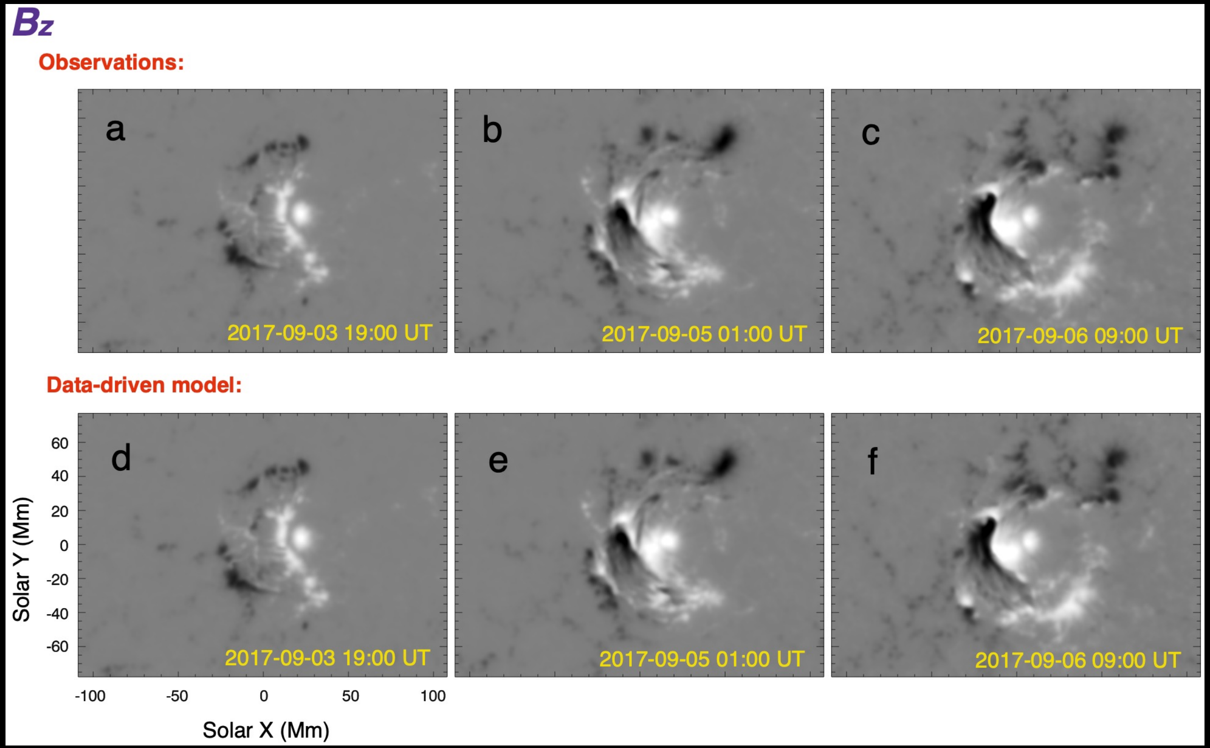

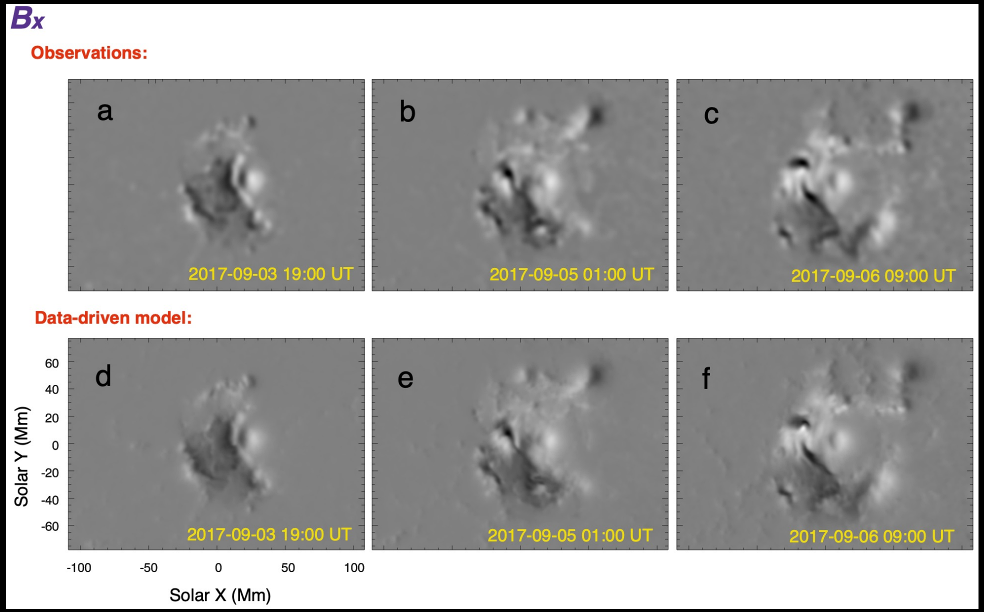

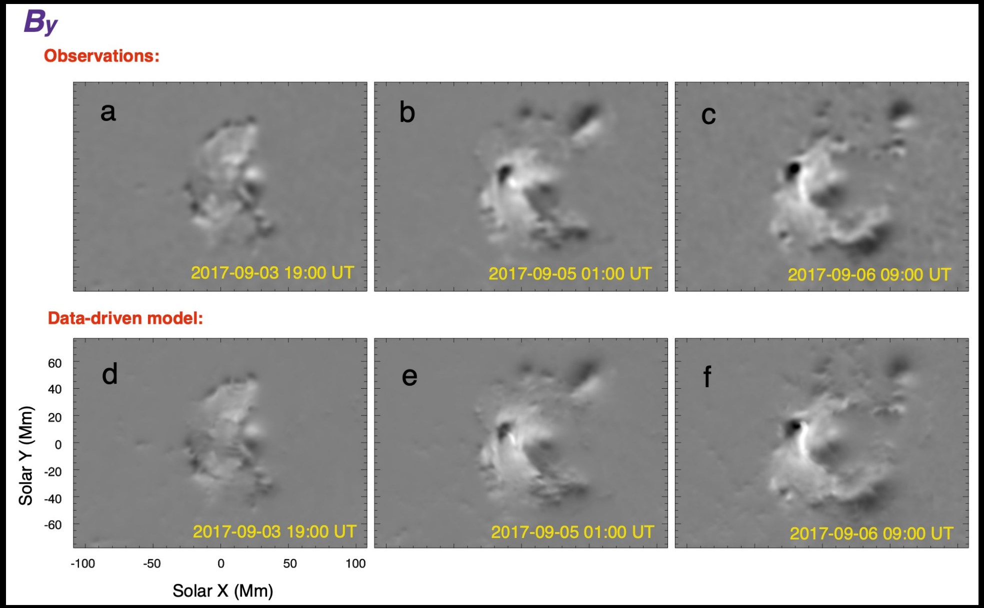

Our data-driven modeling can reproduce the evolution of the photospheric magnetic fields.

Model 5

MHD modeling setup

Quasi-static evolution: Time-dependent magnetofrictional (TMF) model

$$\frac{\partial \boldsymbol{B}}{\partial t} = \nabla \times (\boldsymbol{v} \times \boldsymbol{B} - \eta \boldsymbol{j}),$$

$$\boldsymbol{v} = \frac{1}{\nu} \frac{\boldsymbol{j} \times \boldsymbol{B}}{B^2},$$

$$\nu = \frac{\nu_0}{1 - e^{-z/L}},$$

$$\eta = \eta_0 + \eta_1 \frac{50\zeta}{1 + e^{-(\zeta - 3.0)/0.5}},$$

Uniform resitivity (η_0)

Related to current sheet (η_1 term)

- Simplification of the MHD equations
- Maintain the 3D evolution of the magnetic fields

Such an approach is suitable to model the long-term evolution of the active region

Model 6

MHD modeling setup

Rapid stage: radiative MHD model

$$\frac{\partial \rho}{\partial t} + \nabla \cdot (\rho \boldsymbol{v}) = 0,$$

$$\frac{\partial (\rho \boldsymbol{v})}{\partial t} + \nabla \cdot (\rho \boldsymbol{v}\boldsymbol{v} + p_{tot}\boldsymbol{I} - \frac{\boldsymbol{B}\boldsymbol{B}}{\mu_0}) = \rho \boldsymbol{g},$$

$$\frac{\partial \boldsymbol{B}}{\partial t} + \nabla \cdot (\boldsymbol{v}\boldsymbol{B} - \boldsymbol{B}\boldsymbol{v}) = 0,$$

$$\frac{\partial \varepsilon}{\partial t} + \nabla \cdot (\varepsilon \boldsymbol{v} + p_{tot}\boldsymbol{v} - \frac{\boldsymbol{B}\boldsymbol{B}}{\mu_0} \cdot \boldsymbol{v}) = \rho \boldsymbol{g} \cdot \boldsymbol{v} + H_0 e^{-z/\lambda} - n_e n_H \Lambda(T)$$

$$+\nabla \cdot (\boldsymbol{\kappa} \cdot \nabla T),$$

Energy equation takes into account gravity, empirical background heating, thermal conduction and radiative losses

The ultimate result of the TMF model is served as the initial condition of the radiative MHD model

This complex modeling is used to reproduce the rapid and drastic evolution during the eruption

The above equations are numerically solved by the MPI-AMRVAC (Xia et al., 2018; Keppens et al., 2021, 2023)

Model 7